http://ansinet.com/itj

ITJ

ISSN 1812-5638

INFORMATION TECHNOLOGY JOURNAL

ANSInet
Asian Network for Scientific Information
308 Lasani Town, Sargodha Road, Faisalabad - Pakistan

Information Technology Journal 10 (4): 748-758, 2011
ISSN 1812-5638 / DOI: 10.3923/itj.2011.748.758

Numerical Investigation on the Aerodynamic Characteristics of a Forward Flight Flapping Airfoil with Nonsymmetrical Plunging Motion

Zhang Xingwei and Zhou Chaoying
Department of Mechanical Engineering and Automation, Shenzhen Graduate School,
Harbin Institute of Technology, Xili Shenzhen University Town, Shenzhen 518055, China

Abstract: The aim of this study is to investigate the influence of nonsymmetrical up-down plunging motion of a forward flight airfoil on its aerodynamic characteristics. Numerical simulations are carried out by using the finite volume method to solve the two-dimensional time-dependent incompressible Navier-Stokes equations. To study the influence of an oblique attack angle, the attack angle is selected from -5 to 10 with an increase of 2.5. For each attack angle, seven nonsymmetrical plunging models are examined. The vortex patterns in the wake of the airfoil corresponding to each case are also analyzed and two types of vortex formation are observed where one has two vortices shed in each plunging cycle and the other has four. The vortex pattern in the wake and the moving direction of the vortices are found to be predominantly determined by the plunging motion with different duration time ratio if the frequency and the amplitude of the plunging motion are fixed. It is found that the nonsymmetrical plunging motion alters the time of flow separation at the leading edge compared to the symmetrical one, which may result in higher propulsions. The moving direction of the vortices is also effected by the attack angle of the wing and the variation in the moving direction of the vortices can cause significant changes in propulsion and lift. The present work confirms that both the propulsive and lifting performance of an airfoil can be improved by a nonsymmetrical plunging motion.

Key words: Nonsymmetrical plunge, forward flight, numerical method, aerodynamic forces, vortex patterns

INTRODUCTION

In the nature, birds and insects fly by flapping their wings in the air to obtain enough aerodynamic force to support and propel them. Disclosing the flight mechanisms of these birds and insects can be very instructive for the development of Micro Air Vehicle (MAV). Numerous investigations on the stroke motion of flapping wings of birds or insects in a forward flight have been carried out, such as the studies by Weis-Fogh, (1956), Zarnack (1988), Dudley and Ellington (1990), Tobalske and Dial (1996), Willmott and Ellington (1997), Schilstra and Hateren (1999), Norberg and Winter (2006) and Tian *et al*. (2006) pertaining to aerodynamic forces, control-abilities and propulsive characteristics of the flapping wings. These experimental studies are essential since they are very helpful to explore how the wings delicately move to keep the stability and the flexibility of flight. However, they are limited in revealing the aerodynamic performance of a wing in forward flight since it is not feasible in these experiments to find a representative wing kinematics of the free forward flight. Recently, much effort has gone into the design and construction of devices propelled by flapping such as the MAV with flapping wings, where one of the primary design challenges in these efforts has been the understanding of the unsteady fluid mechanics of flapping.

The generation of thrust by an oscillating airfoil has a notable effect on the structure of the wake. The flow pattern behind a slowly oscillating airfoil consists of a K'arm'an vortex street similar to that behind a bluff body and the sense of rotation of the vortices is a result of the momentum deficit behind the structure corresponding to net drag. Conversely, the wake is inverted and the vortices have the opposite sense of rotation to that behind a bluff body if the airfoil oscillates more energetically, which indicates a jet of fluid behind the airfoil and the development of thrust. Lai and Platzer (1999) performed an experiment of flow visualization on the flow patterns generated by a plunging airfoil. They reported that the vortex patterns generated by the plunging airfoil change from drag-producing wake flows to thrust-producing jet flows as soon as the ratio of

Corresponding Author: Zhou Chaoying, Department of Mechanical Engineering and Automation, Shenzhen Graduate School, Harbin Institute of Technology, Xili Shenzhen University Town, Shenzhen 518055, China
Tel: 0086-755-2603 3866 Fax: 0086-755-2603 2713

maximum plunging velocity to freestream speed exceeds approximately 0.4. Schouveiler *et al.* (2005) experimentally investigated the influences of Strouhal number and the maximum angle of attack on the propulsive performance of a harmonically plunging airfoil. Their results showed that the pattern of the vortices shed in the wake is associated with the behavior of the angle of attack. They also used a bias-angle mechanism to break the symmetry of the foil motion with respect to the flow while the up and down stroke duration times were kept the same. In a biology experimental study, Ennos (1989) filmed some Diptera in free flight using a high-speed cinematography and found that the flow circulations during the two half-strokes were unequal indeed. Also, Park *et al.* (2004) found that the ratio between up-stroke and down-stroke durations of many birds and insects are not the same. It is known that the difference in duration time of up and down strokes plays important roles in the generation of lift and thrust forces. However, the details of how this difference affects the aerodynamic performance of flapping wings are still not fully understood.

Many numerical investigations on an oscillating airfoil have been also carried out. Tuncer and Platzer (1996) investigated the mechanisms of thrust generation for a single flapping airfoil by employing a multiblock Navier-Stokes solver, where the unsteady flow field around the flapping airfoil was analyzed. Their results showed that the propulsive efficiency of a single airfoil can be more than 70% when a flapping amplitude of 0.4 chord length and a reduced frequency of 0.1 are specified. Lewin and Haj-Hariri (2003) numerically examined the flow characteristics and power coefficients of an elliptical airfoil heaving sinusoidally over a range of frequencies and amplitudes. Their simulations produced a periodic and symmetric solution for a given Strouhal number of 0.25. They found that the separation of the leading edge vortices at low heaving frequencies leads to diminished thrust and efficiency and, at high frequencies the efficiency decreases similarly to inviscid fluid. Zhu *et al.* (2008) investigated the aerodynamic performance of dual harmonic flapping airfoils and found that the dual flapping airfoils in a tandem configuration can have better propulsive efficiency than a single flapping airfoil. In above mentioned the numerical studies the duration times for up and down strokes are the same, and none of these numerical studies has discussed the flapping mechanism of a plunging wing consuming different up and down stroke duration times or undergoing a nonsymmetrical plunging motion.

The present study aims to increase the fundamental understanding of aerodynamic performance of a flapping airfoil in a uniform flow undergoing a nonsymmetrical plunging motion. The symmetrical characteristics with respect to the incoming flow is purposely broken and the focus of this study is on the effects of the nonsymmetrical plunge with unequal time between down-stroke duration and up-stroke duration, and the attack angle of the airfoil on thrust, lift and wake structure. Airfoil NACA0014 is considered and the finite volume method is used to solve the governing equation of fluid flow. Only two-dimensional fluid flow is considered. Though in practice the fluid flow around a flapping wing is three dimensional, the present study still will be of fundamental use in exploring the aerodynamic features of a flapping wing undergoing nonsymmetrical motions, and in getting into the physical understanding of creature flying mechanisms.

PROBLEM DESCRIPTION

Physical model: An airfoil undergoing a plunging motion in a uniform flow with a constant attack angle with respect to the uniform flow is considered, which is to simulate a flapping wing in a forward flight. The effective attack angle changes all the time since the airfoil undergoes the plunging motion in a uniform flow. A schematic configuration of the problem is shown in Fig. 1 where a two-dimensional NACA0014 airfoil with chord c of infinite span is employed. α is the attack angle with respect to the uniform flow and $2h_0$ c is twice the amplitude of motion measured from the mean position. U_∞ is the velocity of the uniform flow.

Plunging motion kinematics: The flapping motion of the flying insects includes alternative up-stoke and down-stroke periodic motions and experience different time durations for up and down strokes. It is known that flying insects change the time ratio between down-stroke and up-stroke duration in order to get an alterant force for flight. The plunging motion model employed here with different time ratios between down-stroke and up-stroke durations is concluded from the kinematics analysis of some insects such as desert locust, hawkmoth etc. in a forward flight (Weis-Fogh, 1956; Willmott and Ellington,

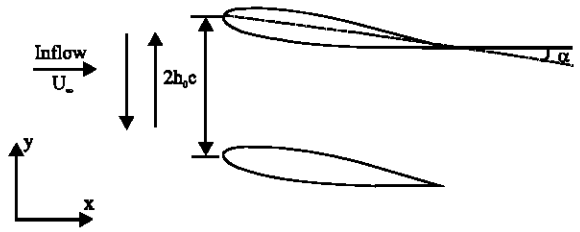

Fig. 1: Schematic configuration of a rigid airfoil undergoing a plunging motion in a uniform flow

1997; Ennos, 1989) and the kinematics equation of the model is extracted from the experimental data of these insects with the fewest number of parameters (see appendix). In this model the plunge displacement h(t) with the plunging period T = 2π/ω can be expressed by the following Fourier equation (Willmott and Ellington,1997)

$$h(t)/c = a_0 + \sum_{n=1}^{m}\left(a_n \cos(n\omega t + c_n) + b_n \sin(n\omega t + d_n)\right) \quad (1)$$

where, a_0, a_n, b_n, c_n and d_n are coefficients of Fourier equation. This model can give a prescribed plunging motion with unequal duration for up stroke and down stroke, and importantly it ensures all the continuities of displacement, velocity and acceleration between different half cycles which can not be ensured by a simple sinusoidal plunging model when an unequal duration time is specified.

A number of cases are examined where for each case the non-dimensional plunging amplitude h_0 is kept at the same value of 0.4. The duration time ratio is defined by:

$$\tau = t_d/t_u \quad (2)$$

where, t_d is the duration time of down stroke and t_u up stroke. Seven different time ratios are selected according to the results of fitting between the available experimental data and the plunging model (1) and they are 0.60, 0.80, 0.82, 1.00, 1.22, 1.26 and 1.68. The detail of how to fit the experimental data with the plunging motion model is described in the appendix. The displacements of the plunging motion for seven different time ratios are illustrated in Fig. 2.

When τ = 1.00, the airfoil will follow a symmetrical down- and up-stroke pattern and the displacement Eq. 1 becomes a sinusoidal function identified as one special Fourier equation where all the coefficients are zero except $a_1=h_0=0.4$.

METHOD OF SOLUTION

Governing equations and solver: The governing equations for unsteady, incompressible and viscous fluid flow can be written in the following form:

$$\nabla \cdot U = 0 \quad (3)$$

$$\frac{\partial U}{\partial t} + \nabla \cdot F = 0 \quad (4)$$

with the two-dimensional Cartesian components, F_{Kj} is given by:

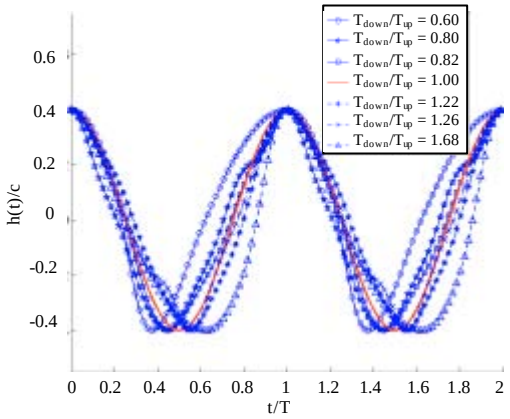

Fig. 2: Kinematics with different down- and up-stroke duration times

$$F_{kj} = \left(U_j - \hat{U}_j\right)U_k + \delta_{jk}P - \frac{1}{Re}\frac{\partial U_k}{\partial x_j} + \overline{u_j u_k} \quad (5)$$

where, $U_j U_k$ is the Cartesian velocity components, $\hat{U}_j$ the mesh velocity, P the pressure and δ_{jK} the Kronecker Delta number. The Reynolds stress tensor $\overline{u_j u_k}$ is given by:

$$\overline{u_j u_k} = \frac{2}{3}k\delta_{jk} - v_t\left(\frac{\partial U_j}{\partial x_k} + \frac{\partial U_k}{\partial x_j}\right) \quad (6)$$

where, v_t is the eddy viscosity determined by the turbulence model and k is the turbulent kinetic energy. The above time-dependent Navier-stokes equation are solved using the finite volume method (Rhie and Chow, 1983; Versteeg and Malalasekera, 1995) and the Shear Stress Transport (SST) k-ω turbulence model is used in the present work. SST as a low Reynolds number model models the Reynolds stress with two transport equations for the turbulent kinetic energy and the specific dissipation rate ω, respectively. The wall functions are not used. One can refer to Menter (1993) for a detailed description of the SST model. The Pressure Implicit with Splitting of Operators (PISO) algorithm (Issa, 1985; Issa *et al*., 1991) is employed to deal with the coupling between the pressure and velocity. The third-order accurate QUICK scheme (Leonard, 1979) is used to discrete the convective terms. These numerical algorithms are quite standard now.

The total computational domain is 18c long and 10c wide. A conformal-hybrid grids system that consists of quadrangular meshes in an internal domain around the airfoil and triangular meshes in an outer field is used as shown in Fig. 3. The complete inner mesh moves according to the wing kinematics and a dynamic deformable remesh method in accordance with Geometric

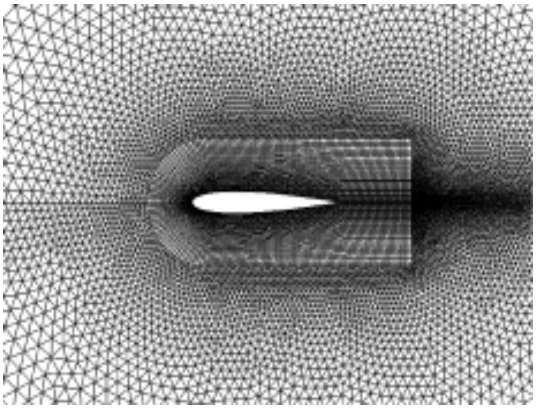

Fig. 3: Computational grid around the plunging airfoil

conservation law method (Lesoinne and Farhat, 1996) is used in the outer field. A series of tests for grid independent and time step independent were conducted before actual calculations were carried out. Based on these tests, element number about 4.2×10^4 and time step 0.0025T are selected for all the cases.

The incoming flow runs from the left to the right. At the inlet of the computational domain, a uniform profile is prescribed:

$$U=U_\infty \tag{7}$$

The right outlet is far away enough so that a boundary condition of fully developed flow is given, i.e.,

$$\frac{\partial U}{\partial x}=0 \tag{8}$$

The no-slip boundary condition is specified at the airfoil surface and a symmetry boundary condition (Elhadi *et al*., 2002) is applied at the lateral faces of the computational domain. The influence of this symmetry condition has been investigated and found to be sufficiently adaptive. The simulation starts assuming the fluids is initially at rest.

Important parameters: The Reynolds number, which characterizes the effects of viscous, is defined as:

$$Re = \rho U_\infty c/\mu \tag{9}$$

where, ρ is the density of fluid and μ the dynamic viscosity.

The Strouhal number, which characterizes the periodicity in a flow field, is defined as:

$$St = 2h_0cf/U_\infty \tag{10}$$

where, f is the frequency of plunging motion.

The reduced frequency is defined as:

$$k = \omega c/U_\infty \tag{11}$$

For all calculations, the Reynolds number is set at 10^4 and the reduced frequency is kept at 2 which results in a Strouhal number of 0.255.

The lift and drag coefficients are computed from:

$$C_l=\frac{2F_y}{\rho csU_\infty^2}, C_d=\frac{2F_x}{\rho csU_\infty^2} \tag{12}$$

where, s is the surface area per unit spanwise length of the airfoil and F_y and F_x are instantaneous lift and drag forces, respectively. These forces are calculated from the integration of the pressure and the viscous force on the surface of the airfoil.

The period-averaged thrust and lift can be evaluated as:

$$\overline{F}_{Th}=-\frac{1}{T}\int_0^T F_x(t)dt \tag{13}$$

$$\overline{F}_L=\frac{1}{T}\int_0^T F_y(t)dt \tag{14}$$

where, $F_x(t)$ and $F_y(t)$ represent the instantaneous force components in x and y directions respectively. Then, the mean vertical force coefficient C_V is defined as:

$$C_V=\frac{2\overline{F}_L}{\rho csU_\infty^2} \tag{15}$$

The mean thrust coefficient C_{Thm} is defined as:

$$C_{Thm}=\frac{2\overline{F}_{Th}}{\left(\rho U_\infty^2 cs\right)}=\frac{1}{T}\int_0^T(-C_d)dt \tag{16}$$

RESULTS AND DISCUSSION

Validation: A series of validation tests for the computation code are conducted before actual calculations are carried out and the results are compared with related experimental and numerical results published in the literature. One of the comparisons is shown in Fig. 4 where the time history of the drag coefficient for the airfoil plunging in the uniform flow with τ =1.00, α = 0, k = 2, St = 0.255 and Re = 10^4 is plotted against the dimensionless time $t' = tU_\infty/c$. It is seen that the result agrees well with the results of Tuncer and Kaya (2003)

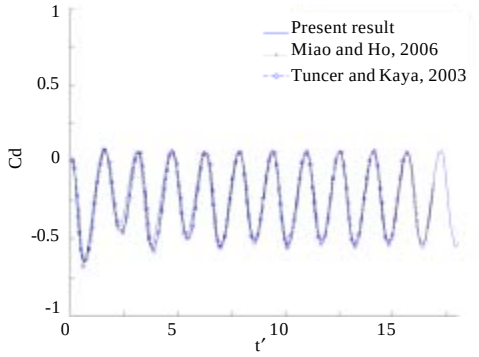

Fig. 4: Comparison of the drag coefficient time histories

and Miao and Ho (2006) for the same problem when the flow settles down to a steady state at around $t' = 6$ from an impulsive start.

The vorticity contours around the airfoil for the times of t/T = 0.25, 0.5, 0.75 and 1.00 are illustrated in Fig. 5a-d, respectively. During the down stroke (Fig. 5a, b), the clockwise vortex filaments roll up into a large leading edge vortex on the upper side of the airfoil and the counterclockwise vortices produced by last half cycle truncate the vortex band at the tailing edge (Fig. 5c, d). Then the truncated vortex advects to downstream (Fig. 5d). During the up stroke, similar process repeats and the counterclockwise vortices gradually grow up and roll up into a large vortex on the lower side of the airfoil. The alternatively shed vortices form a vortex street in the downtream of the airfoil similar to that behind a bluff body. However, the difference is that the counterclockwise vortices here are in the upper line of the street while the clockwise vortices in the lower line, which indicates that the wake is inverted and the vortices have the opposite sense of rotation to that behind a bluff body. Consequently, thrust rather than drag is generated. The present reverse Von Karman vortex street formed behind the plunging airfoil is in agreement with the experimental observation of Von Karman and Burgers (1935).

Overall comparison on forces for the plunging cases: To investigate the effects of nonsymmetrical characteristics on the aerodynamic performance of the airfoil, seven attack angles ranged from -5° to 10° with an increase of 2.5° are examined for each time ratio. The variations of the period averaged values of thrust coefficient, vertical force coefficient with the attack angle are studied. Normally a period averaged value is calculated over ten cycles of the plunging motion after a steady status is reached.

Figure 6 shows the variation of C_{Thm} with angle α for seven different values of τ where α is ranged from -5° to 10° with intervals of 2.5°. It is seen immediately from the figure that when the attack angle α is zero, an asymmetrical plunging motion of the airfoil produces larger average thrust than the symmetrical one (i.e., the balck unmarked curve in Fig. 6) and the average thrust reaches a maximum value at both $\tau = 1.62$ and 0.60. For each fixed α, there is at least one nonsymmetrical plunge can provide a higher thrust than the symmetrical plunge. Moreover, the way of the average thrust C_{Thm} varying with α is different for different values of τ, which indicates that whether one asymmetrical stroke motion produces higher thrust than the symmetrical case is also affected by the attack angle α. An appropriate combination of τ and α will generate a better thrust, for example, when the airfoil plunges in an asymmetrical stroke motion with $\tau = 0.60$ and $\alpha = 5°$, it will generate the highest thrust for the cases considered. The attack angle α with respect to the incoming flow can modify the thrust to make the flight speed up, slow down or uniform. This is consistent with the observation on hawkmoths by Willmott and Ellington (1997) where they found that the increases in forward flight speed of the hawkmoths always tended to be accompanied by an increase in their stoke plane angle and a decrease in their body angle which results in a change in the attack angle with respect to the incoming flow.

The mean vertical force coefficient is plotted as a function of α in Fig. 7. It can be seen that the vertical force produced by the symmetrical motion increases with α almost linearly, while for the nonsymmetrical cases, the force dose not always increase monotonically. As an example, for the nonsymmetrical case of $\tau = 0.80$, the force increases first and reaches a maximum value at $\alpha = 2.5°$, and then decreases. Figure 7 also shows that the nonsymmetrical character with different ratios between the down and up stroke duration has a significant effect on the generation of vertical force when the forward flight airfoil plunges with a fixed inclination. For the practical forward flight, the positive mean vertical forces can be used to offset the payload or provide an ascending flight, while negative mean vertical forces will cause the flight moving downward. Form the above results, it can be seen that the aerodynamic forces can have many varieties of change by adjusting the nonsymmetrical character of wing motion no matter the attack angle changes or not. These results indirectly explain why most stoke motions of the flying insects are nonsymmetrical patterns.

Figure 8 shows the ratio of mean vertical force coefficient to mean thrust coefficient versus the time ratio τ. The ratio $\eta = C_v/C_{Thm}$ can be one of criteria to assess the performance of the flapping flight. In order to facilitate comparison the symmetrical plunge motion with $\tau = 1.00$ is chosen as the baseline in the discussion. It can be seen that there is at least one nonsymmetrical plunge that can

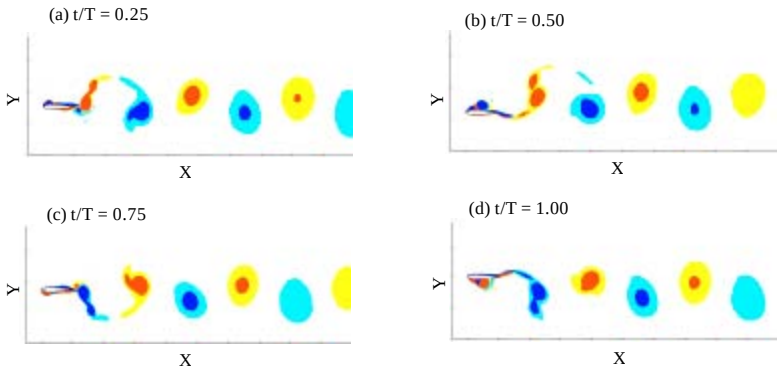

Fig. 5: (a-d) Vorticity contours for a symmetry plunge motion with α = 0; (blue: clockwise; red: counterclockwise)

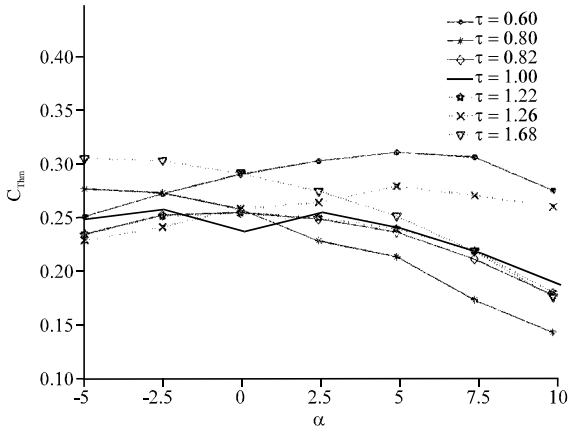

Fig. 6: The period-averaged thrust coefficients with respect to angle α computed at k = 2

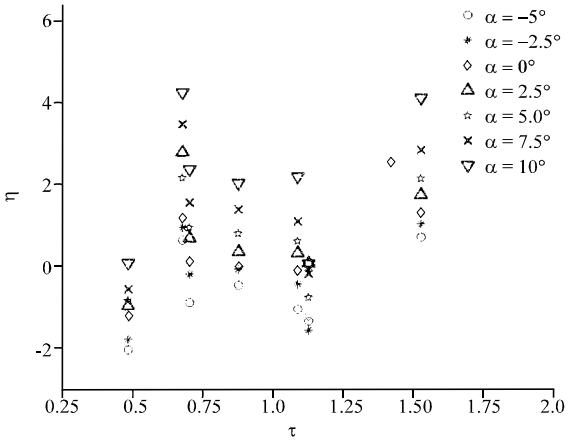

Fig. 8: Variations of ηwith respect to time ratio τ. between down- to up-stroke

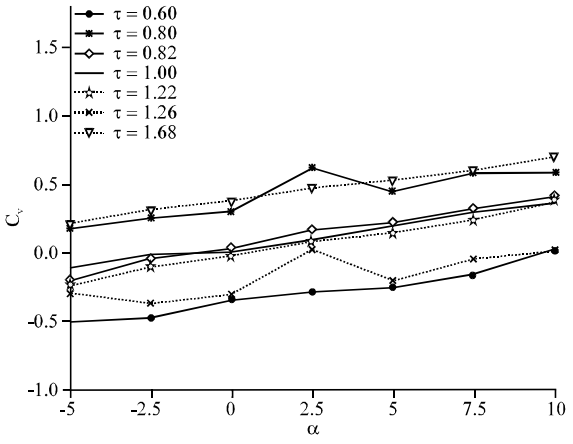

Fig. 7: Variations of averaged vertical force coefficients withα for different values of τ

carry more loads during the uniform flight at a fixed attack angle. For an example, when α is kept at 10°, the nonsymmetrical plunge with τ = 0.80, 0.82, 1.22 and 1.68 provide bigger values in mean vertical force coefficient to mean thrust coefficient ratio than the case τ = 1.00. However, not all the nonsymmetrical plunges provide good performance assessed by the mean vertical force coefficient to mean thrust coefficient ratio (e.g. τ = 0.60).

Wake structures of nonsymmetrical plunge between down- and up- stroke: To further analyze the effect of nonsymmetrical plunging motion on the aerodynamic performance of an airfoil, the vorticity structures in the wake of the airfoil undergoing a plunging motion with a constant attack angle with respect to the incoming flow but different time ratio of down- and up-stroke duration are illustrated in Fig. 9a-f. Though the vortex shedding patterns are definitely different for different values of τ, it can be seen that the reverse Von Kármán street pattern persists in every present result, although largely weakened in some case. Both symmetrical and nonsymmetrical stroke patterns produce a positive mean thrust as indicates by Fig. 6.

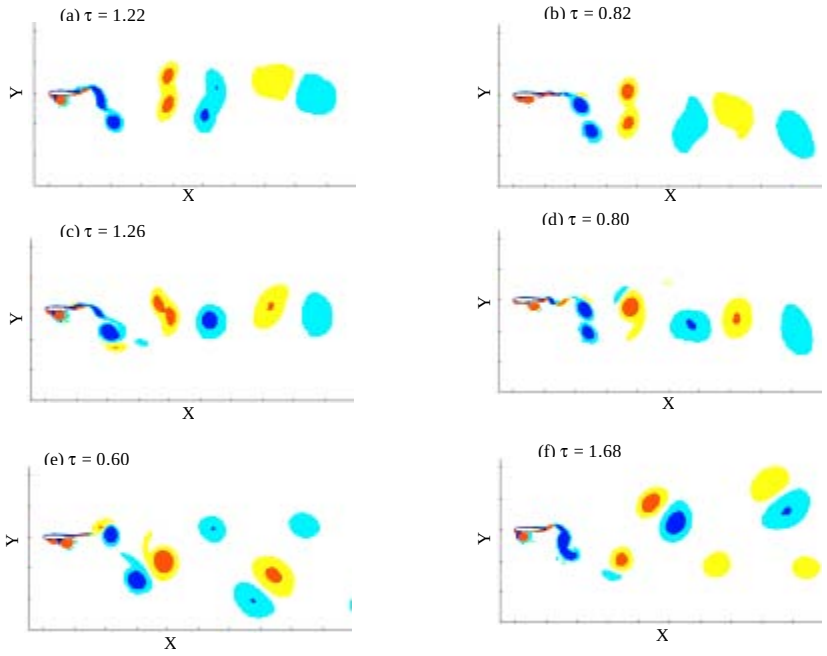

Fig. 9: (a-f) Vorticity contours for nonsymmetry plunge with different down-up time ratio when $\alpha = 0°$ and $kh_0 = 0.8$. (blue: clockwise)

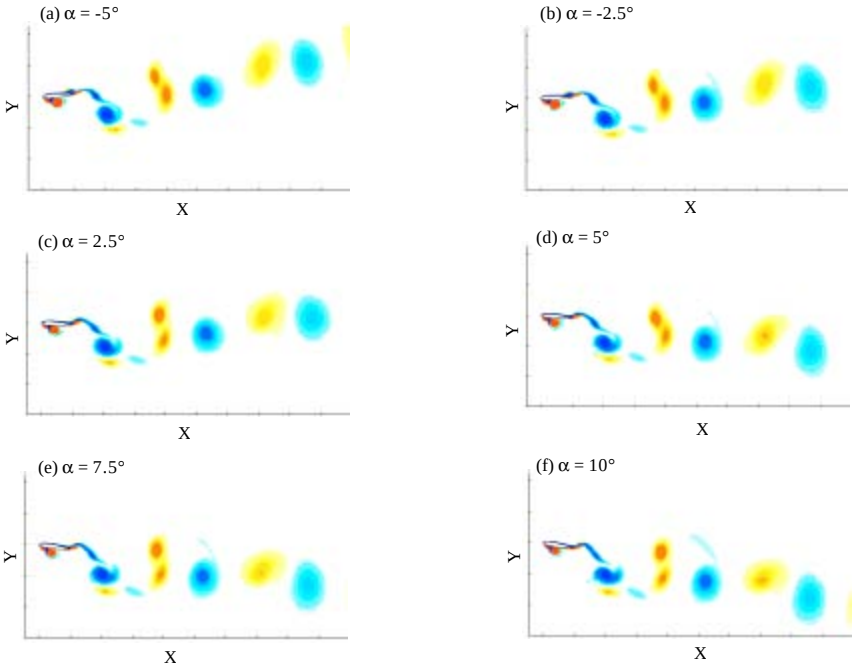

Fig. 10: (a-f) Vorticity contour for nonsymmetry plunge with $\tau = 1.26$ when the airfoil at highest position. (blue: clockwise)

Current results also show the wake pattern of the airfoil is determined by the formation and the growth of both the LEV and the TEV and also the interaction between them. The timing of the separation of the Leading-edge Vortex (LEV) and Trailing-edge Vortex (TEV) is closely similar for one nonsymmetrical motion.

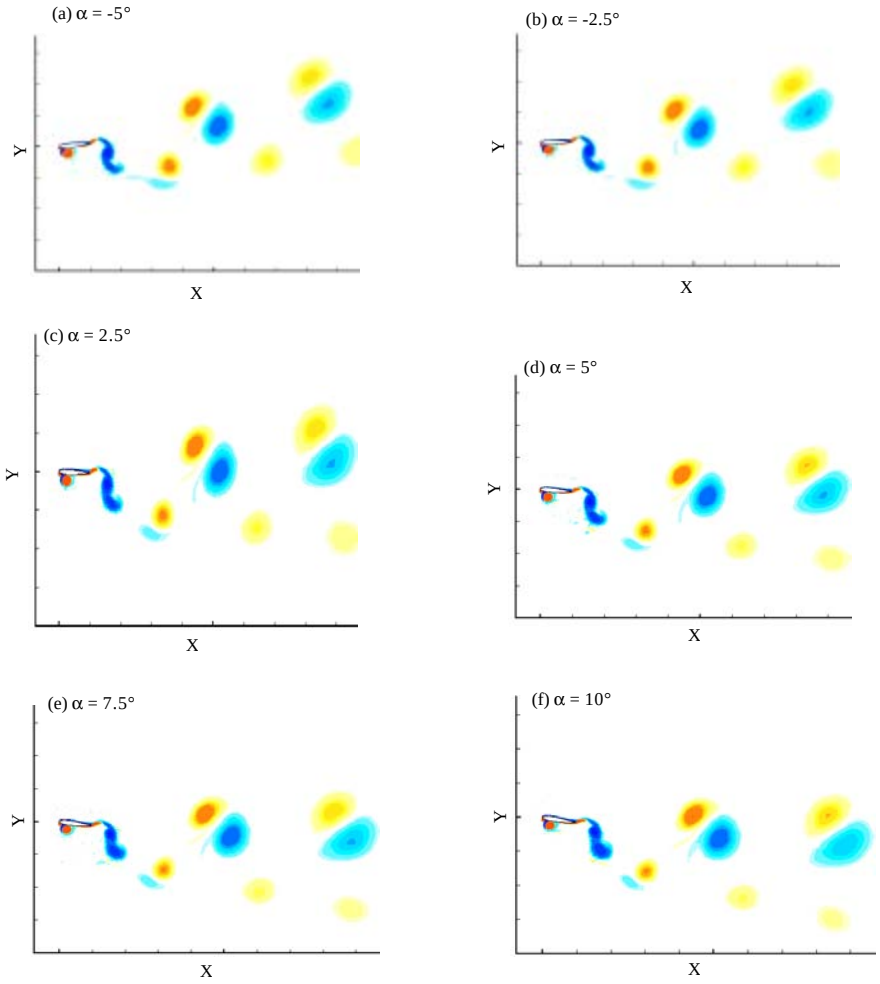

Fig. 11: (a-f) Vorticity contour for nonsymmetry plunge with τ = 1.68 when the airfoil is at highest position. (blue: clockwise)

Once the motion is determined, the corresponding pattern of vortex street resulted from the fate of LEV and TEV could be existent. As an example, for the case with τ = 1.26 (Fig. 10a-f) the shedding mechanisms of the vorticity is the same expect the transfer direction of the vortex street. There is a little difference in the second shed off vortex in upper branch of the vortex street (Fig. 10α = -5°, 7.5°), which is evidence for the intensity of the LEV weakly affected by the α.

Besides the vortex pattern in the wake, the trend of vortex street is also decided by the plunge pattern. When α = 0°, the trend of street produced by the symmetrical plunge motion is level. Nevertheless, the vortex street of the nonsymmetrical patterns deflected a little from the level which result that the mean vertical force coefficients is nonzero as shown in Fig. 6a. A similar deflection of the street was experimentally observed by Lai and Platzer (1999) at a larger St (St>0.6) using a sinusoidally symmetrical plunge.

For each nonsymmetrical plunging motion, the angle of attack also has a significant affect on the trend of the vortex street. Figure 10 shows the vortex street with τ = 1.26 for different values of α ranging from -5° to 10° in an interval of 2.5°. The vortex structure in the wake are closer the same except the inclination of the vortex street. When the vortex street is downward-sloping the higher mean vertical force could be produced such as the case with α = 5° provide 44% lift higher than the α = -5° case. When the trend of the street near to the level, the bigger mean thrust appears such as the case with α = 5 ° provide 18.4% thrust higher than that one when α = -5°. Additional, it can be found that the intensity of the second shed vortex in the near rear region has a slight change as the angle α increases.

Additionally, it should be noted that there are different formations of shedding vortices per cycle in the vortex street when $\alpha = 0°$ as shown in Fig. 9. For a symmetrical plunging motion, there are two vortices shed from the airfoil per cycle whereas for a nonsymmetrical plunging motion with a fixed reduced frequency and amplitude, there may be two or four vortices shed per cycle. Figure 11a-f show that there are four vortices shed in to the wake per cycle when $\tau = 1.68$. It can be considered that there are two tiers of the streets after the rear of the wing. The distribution of two tiers located upper and lower respect to the centerline of wake. The LEV pairs up with the TEV but the two do not immediately merge which result in a much wider wake than those in the other cases. Lewin and Haj-Hariri (2003) found a similar but not the same format in the vortex street at $kh_0 = 1.0$ and a higher reduced frequency with the symmetrical plunge motion. Their results show that the location of two tiers is symmetrical about the mean position of the wake when α is zero. While our shedding format is also four-vortices, the distribution of the tow tiers is not symmetrical respect to the mean position of wake and the difference in vortex intensity between the two tiers exists either. This asymmetric distribution makes the mean thrust get higher values at small attack angles (Fig. 6). When the stronger tier locates in the upper side of wake, a higher mean vertical lift appears. Such as the nonsymmetrical pattern with $\tau = 1.68$ provides higher mean values both lift and thrust. Whereas, the weaker tier locates in the upper, the mean vertical lift attain a lower value (e.g., $\tau = 0.6$).

The above results reveal that fate of the LEV and TEV is mainly determined by the motional pattern and the strength of the LEV and TEV is weakly affected by the attack angle. The propulsive force decided by the formation of the wake structure which results from the development of the LEV and the TEV. Whether the plunging pattern is symmetrical or not has the predominant effect on the formation of vortex street in the wake. Summarizing, the nonsymmetry moving patterns used by the flying bio is one of significantly factor to improve the performance of forward flight. These lead to the suggestion that the flapping vehicles may adopt sets of nonsymmetrical plunging motion with different time ratios between downstroke and upstroke during to improve the thrust performance and level the loads over the forward flight.

CONCLUSIONS

A comprehensive numerical simulation for a NACA0014 airfoil stroking up and down in a uniform flow has been carried out using the finite volume method. The flow is assumed to be two-dimensional, the Reynolds number is kept at 10^4 and the reduced flapping frequency is set at 2. In particular, the nonsymmetrical characteristics caused by the time ratio between the down and up stroke duration have been studied. The lift, thrust, lift-to-thrust ratio have been computed to assess the nonsymmetrical effects on the forward flight. The corresponding wake structures of the airfoil have been analyzed. It has been shown that the nonsymmetrical motion indeed can enlarge lift, thrust or even both of them during the forward flight. Further, current numerical results confirm that the nonsymmetrical motion of insect wings plays an indispensable role during their flight and can make their flight much more effective and flexible.

Present results show that all the period-averaged thrusts are positive for the cases studied and a reversed Von Karman vortex street always exists for both symmetrical and nonsymmetrical plunging motions. For the cases with unequal duration time between down- and up-stroke, there always exists at least one nonsymmetrical plunging motion which produces much bigger mean thrust or vertical mean force than the symmetrical motion. This has a close relationship with the formation of the vortex street. The nonsymmetrical plunging motions adjust the development of the LEV and TEV, and also the interaction between them, which results in the changes in the formation of the vortex street in the wake of the plunging airfoil. The trend of this reverse Von Karman street is found to be also affected by the attack angle for both symmetrical and nonsymmetrical plunge.

Two types of vortex pattern in the wake have been observed. One has two vortices shed in each plunging cycle and the other has four. For the wake with two-vortices shed per cycle, higher mean vertical lifts will be produced when the vortex street advects downwards. When the trend of the wake is near to the level, a higher period-averaged thrust appears. Also, both the symmetrical and nonsymmetrical plunging motion can produce the four-vortices shed pattern in the wake, but the detailed distribution is different. When the attack angle is zero, two tiers of vortices locate after the airfoil symmetrically above and below the mean position. However, the situation for the nonsymmetrical plunging motion is quite different. Apart from the nonsymmetrical location of the two tiers, the vortex intensity between the two tiers is also different. The difference in the intensity of the vorticity between two tiers implies that the half stroke which spends longer time produces a weaker LEV and TEV.

Current study focuses on heaving pattern not considering the pitching model. For the simulative conditions mentioned above, the moving pattern is

prerequisite to the characteristics of flow field around the plunging wings. For one of prescribed patterns, the Strouhal number, heaving amplitudes and oblique angles have the significant influence on the vortex shedding mechanism of plunging wing. The nonsymmetrical plunging motion is one of significant factors to improve the performance of the vehicles. This leads to the suggestion that the flapping vehicles may use the nonsymmetrical character of motion to alter the thrust and level the loading by adjusting the time ratio between up and down stroke duration over the forward flight. Present work emphasizes the unsteady effects and the results can be of help for the development of flapping vehicles assembled the bionical actuator and its controller. Future studies perhaps will dconsider the effect of deformation caused by load distribution along the wing surface and computation on the three-dimensional rigid model need to be further performed.

ACKNOWLEDGEMENTS

The study described in this research was conducted in Shenzhen Graduate School, Harbin Institute of Technology and fully supported by a grant from National Natural Science Foundation of China (Project number No. 90715031). The financial support is gratefully acknowledged.

APPENDIX

For completeness we briefly describe the main method of dealing with the stroke kinematics spending different time between up and down half-stroke. Take one case when the time ratio $\tau = 1.26$ as an example. Willmott and Ellington (1997) filmed the course of wingbeats of a Hawkmoth spending different time between downstroke and upstroke using high-speed video system in an open-jet wing tunnel. The experimental displacement is fitted in a form of Fourier series as Eq. 1 as shown in Fig. 12a. The first and second derivative of Fourier equations is reasonable continuous, which ensure that the adjustments on the velocity and acceleration are always continuous. In order to transform the amplitude of the curve, the conversion factor has been used. Then, through the translation to ensure that the downstroke begin at the upper branch of the amplitude. Resultant figure is depicted in Fig. 12b. Another, in order to further investigate, a nonsymmetrical plunge with $\tau = 0.80$ was constructed by mean of turning the displacement of case with $\tau = 1.26$. The plunging model with $\tau = 1.26$ spend the same time during downstroke with the case with $\tau = 0.80$ in the upstroke cycle. The treatment

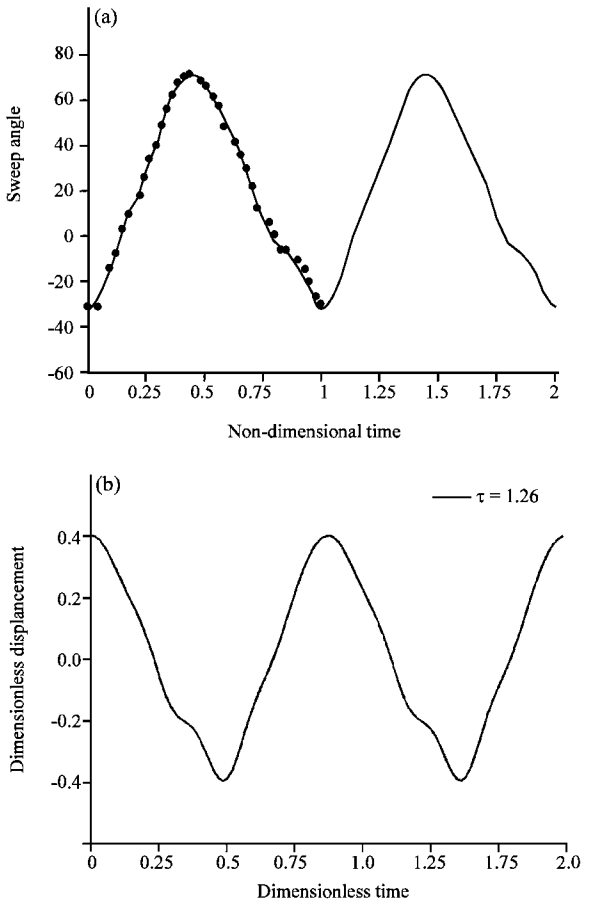

Fig. 12: (a) The fitted curve of a Fourier series when the time ratio of downstroke to upstroke during is 1.26 and (b) the dimensionless displacement of the model at $\tau = 1.26$

of the other unsymmetrical patterns such as $\tau = 1.22, 0.82$ and $\tau = 1.68, 0.60$ is in the same methods and the dimensionless displacements of the plunging are shown in Fig. 2.

REFERENCES

Dudley, R. and C.P. Ellington, 1990. Mechanics of forward flight in bumblebees: I. Kinematics and morphology. J. Exp. Bio., 148: 19-52.

Elhadi, E.E., L. Xiaosong and W. Keqi, 2002. Numerical simulation of 2D separated flows using two different turbulence models. J. Applied Sci., 2: 1057-1062.

Ennos, A.R., 1989. The kinematics and aerodynamics of the free flight of some diptera. J. Exp. Biol., 142: 49-85.

Issa, R.I., 1985. Solution of the implicitly discretized fluid flow equations by operator-splitting. J. Comput. Phys., 62: 40-65.

Issa, R.I., B. Ahmadi-Befrui, K.R. Beshay and A.D. Gosman, 1991. Solution of the implicitly discretized reacting flow equation operator-splitting. J. Comput. Phys., 93: 388-410.

Lai, J.C.S. and M.F. Platzer, 1999. Jet characteristics of a plunging airfoil. AIAA J., 37: 1529-1537.

Leonard, B.P., 1979. A stable and accurate convective modelling procedure based on quadratic upstream interpolation. Comput. Meth. Applied Mechan. Eng., 19: 59-98.

Lesoinne, M. and C. Farhat, 1996. Geometric conservation laws for flow problems with moving boundaries and deformable meshes and their impact on aeroelastic computations. Comp. Meth. Applied Mechan. Eng., 134: 71-90.

Lewin, G.C. and H. Haj-Hariri, 2003. Modelling thrust generation of a two-dimensional heaving airfoil in a viscous flow. J. Fluid Mech., 492: 339-362.

Menter, F.R., 1993. Zonal two-equation k–w turbulence models for aerodynamic flows. AIAA 24th Fluid Dynamics Conference, Orlando, FL, USA.

Miao, J.M. and M.H. Ho, 2006. Effect of flexure on aerodynamic propulsive efficiency of flapping flexible airfoil. J. Fluids Struct., 22: 401-419.

Norberg, U.M.L. and Y. Winter, 2006. Wing beat kinematics of a nectar-feeding bat, Glossophaga soricina, flying at different flight speeds and Strouhal numbers. J. Exp. Biol., 209: 3887-3897.

Park, H.C., S.Y. Lee, S.M. Lim, S.K. Lee, K.J. Yoon and N.S. Goo, 2004. Design and demonstration of flapping wing device powered by LIPCA. Proc. SPIE, 5390: 212-216.

Rhie, C.M. and W.L. Chow, 1983. Numerical study of the turbulent flow past airfoil with trailing edge separation. AIAA J., 21: 1525-1532.

Schilstra, C. and J.H. Hateren, 1999. Blowfly flight and optic flow. I. Thorax kinematics and flight dynamics. J. Exp. Biol., 202: 1481-1490.

Schouveiler, L., F.S. Hover and M.S. Triantafyllou, 2005. Performance of flapping foil propulsion. Fluids nd Struc., 20: 949-959.

Tian, X., J. Iriarte-Diaz, K. Middleton, R. Galvao and E. Israeli et al., 2006. Direct measurements of the kinematics and dynamics of bat flight. Bioinspir. Biomim., 1: 10-18.

Tobalske, B. and K. Dial, 1996. Flight kinematics of black-billed magpies and pigeons over a wide range of speeds. J. Exp. Biol., 199: 263-280.

Tuncer, I.H. and M. Kaya, 2003. Thrust generation caused by flapping airfoils in a biplane configuration. J. Aircraft, 40: 509-515.

Tuncer, I.H. and M.F. Platzer, 1996. Thrust generation due to airfoil flapping. AIAA J., 34: 324-331.

Versteeg, H.K. and W. Malalasekera, 1995. An Introduction to Computational Fluid Dynamics: The Finite Volume Method. Wiley, New York.

Von Karman, T. and J.M. Burgers, 1935. Aerodynamic Theory. Springer, Berlin, pp: 280-310.

Weis-Fogh, T., 1956. Biology and physics of locust flight. IV. Notes on sensory mechanisms in locust flight. Bio. Sci., 239: 553-584.

Willmott, A.P. and C.P. Ellington, 1997. The mechanics of flight in the hawkmoth Manduca sexta. I. Kinematics of hovering and forward flight. J. Exp. Bio., 200: 2705-2722.

Zarnack, W., 1988. The effect of forewing depressor activity on wing movement during locust flight. Bio. Cybernet., 59: 55-70.

Zhu, B.L., T.H. Xiao, H.S. Ang and X.C. Zhou, 2008. Propulsive effects of same frequency dual flapping a airfoils in a micro air vehicle. J. T Singhua Uuiv., 48: 298-301.